Available online at www.sciencedirect.com

ScienceDirect

Procedia Computer Science 126 (2018) 186–194

Procedia Computer Science

www.elsevier.com/locate/procedia

International Conference on Knowledge Based and Intelligent Information and Engineering Systems, KES2018, 3-5 September 2018, Belgrade, Serbia

Automatic CORINE land cover classification from airborne LIDAR data

Jesús Balado[a]*, Pedro Arias[a], Lucía Díaz-Vilariño[ab], Luis M. González-deSantos[a]

[a]*Applied Geotechnologies Group, Dept. Natural Resources and Environmental Engineering, School of Mining and Energy Engineering, University of Vigo, Campus Lagoas-Marcosende, CP 36310 Vigo, Spain*

[b]*Dept. Civil Engineering, University of Porto, s/n, R. Dr. Roberto Frias, 4200-465 Porto*

Abstract

Point clouds provide valuable information that is not contained in satellite or aerial images. In this work, the potential of airborne LIDAR data for automatic land cover classification following the CORINE standard is evaluated. The methodology consists on the ordering of the point clouds by means of grid maps and rasterized for their use in the training of a Deep Learning classifier model ResNet-50. Three exclusive features of this type of information are extracted: height difference between points, average intensity and number of returns. The methodology has been tested in one case study at level 1 of CORINE inventory, reaching a 73.5% accuracy and a 59,8% Cohen Kappa coefficient. The main confusion occurs between types with strong similarities.

Keywords: point cloud, laser scanner, urban, ResNet-50, convolutional neural networks, machine learning, dimensionality reduction, feature extraciotn

1. Introduction

Land monitoring allows a better harnessing of the land. It provides valuable information about the environment, as flows of raw materials from production areas (agricultural and forest lands) to consumption areas (urban and industrial lands). This favors the design of policies that improve the production, transport or conversion of land use. In addition, land monitoring through the years allows to determine the local evolution of the environment [1] and predict future use [2]. Population changes are easy to predict because they occur in a phased manner over time. The most common are the increase in population (urban and rural increase, or conversion from rural to urban areas), depopulation (conversion of rural to forest and barren lands) and the abandonment of farmlands. Abrupt changes, such as deforestation (either for crops or caused by fires) or reforestation are more difficult to prevent because they depend on decisions and accidents that take place at a specific moment.

10.1016/j.procs.2018.07.222

The CORINE (Coordination of Information on the Environment) project begins in 1985 as an initiative of several countries of Europe in order to create a land cover structure on the state of the soil and monitor areas of environmental interest [3]. After the first inventory in 1990, periodic updates have been made to monitor environmental changes in 2000, 2006 and 2012 [4], [5]. For the realization of the inventory, the use of satellite images is recommended since the cost and time of acquisition per square meter is less than in other methods. The land cover classification for the CORINE program is done manually, although some countries already implement a semiautomatic mode.

Traditionally, the land classification was done manually, either through aerial-satellite photographs or in the field. Subsequently, the automatic classification began to be used based on color features and patterns in the images [6]. The recent Deep Learning techniques allow an automatic classification with greater accuracy than traditional techniques, even than the application by the manual human user [7].

Although the land classification is well studied on image data, even with Deep Learning [8], [9], the same does not happen on LIDAR data. This may be due to the fact that their use for these applications is more recent, that laser sensors do not have enough resolution or that the computational cost necessary to process point clouds is much greater than that of processing images. Even so, laser scanner technology can help the classification process with 3D information, which images do not possess, and information added to the laser beam as the reflectivity of the element and the number of returns.

The objective of this work is the design and testing of a methodology for the automatic land cover classification from airborne LIDAR data based on CORINE inventory. The methodology begins with the ordering of the point cloud for the creation of fixed-size samples. The feature extraction is done through a rasterization that assigns to each channel of the resulting image a value: R - height difference, G - medium intensity and B - number of returns. These sample images are used to train a neural network ResNet-50. The methodology is applied to a case study. The land cover types used in this work are three (artificial surfaces, agricultural areas, and forest and semi-natural areas). They correspond to level 1 of the CORINE land cover classification. They correspond to level 1 of the CORINE land classification. Levels 2 and 3 have a very low number of unbalanced samples for training a neural network due to a high land fragmentation.

This paper is organized as follows. Section 2 collects related work about land cover classification using from LIDAR data. In Section3, the proposed methodology is explained. Section 4 analyses the results of the application of the methodology in one case study. Finally, Section 5 concludes this work.

2. Related Work

As noted above, point clouds for land cover (or land use) classification are not as well used as images. Even so, there are some works that use this information, either in isolation or together with images, compensating the weak points of each information [10]. Kunwar et al. [11] he quantify a 32% increase in accuracy compared to joint use with the use of LIDAR data alone, but these percentages vary greatly with methodologies and case studies. Data can be processed through a succession of operations and manual classifications, such as the one used by [12] to differentiate grass, trees, roofs and their shadows; or simply used to train a machine learning system. Koetz et al. [13] implement a SVM classifier with LIDAR and images features for a land cover classification. It is also very common to use products generated from point clouds, such as Digital Terrain Model [14] or Digital Surface Model [12] and do not directly load the cloud over the classification process. The joint classification of LIDAR data and images can be done pixel by pixel, point by point, object-based, although some authors work with other classification units, such as urban parcels [15].

Regarding the works that use as input only point clouds. Chehata et al. [16] study 21 different features extracted from the point cloud. Their features can be grouped into five types: height-based, echo-based, eigenvalue-based,

plane-based and FW features. Their objective is the classification of urban areas artificial ground, building, natural ground and vegetation. Their conclusion is that the most relevant feature for all classes is the height difference and echo-based attributes seem to be non-relevant. Another study of an urban classification is carried out by [17]. They focus on the differentiation between tree canopies and buildings, using the elevation and intensity difference between the first and last return of the laser. Yoon et al. [18] use the intensity of the LIDAR data exclusively, evaluating if with this information it is possible to replace the infrared layer of the images. The author outlines the large standard deviation that has the intensity of vegetation points and that intensity does not provide enough separability among land cover classes. Antonarakis et al. [19] implement intensity and height as features to perform an object-based land cover classification. They are able to make a distinction between forest types based on the distribution of points on the Z axis, showing clearly differentiated histograms for natural forests and different plantings according to their age. Another author who implements these features (intensity and height) is [20]. In his results, he argues that the accuracy was better than those using multispectral imagery alone and the object-based approach being better than pixel based on land cover classification.

Unlike other works [16], [20], in this work it is not possible to use a pixel-based, point-based or object-based classification, where the pixel with similar characteristics are grouped [12], it is not possible to apply other methods to this type of problem. Within each CORINE land type, the existing pixel-points present important variations and can belong to elements more typical of other land types. For example, it is common the existence of trees and low vegetation between fields, without this supposes the existence of a land type forest, or the existence of isolated roofs does not mean an urban area. Because of this, the classification is implemented at regular intervals of the point cloud, which are then rasterized and used to train the Deep Learning classifier, once its features (difference in height, average intensity and number of returns) are saved in pixels.

3. Methodology

The methodology is divided into two parts: sample generation, which includes ordering of the point cloud and feature extraction, and the deep learning training/classification process.

3.1 Sample generation

Images are needed to use a trainer/classifier based on Deep Learning. This subsection describes how these images are generated from ALS point clouds. Images for training the neural network must have a fixed size NxN. The image must have enough pixel-features that allow a correct classification of the sample. But in turn, it should be as small as possible to minimize the approach error that occurs when coexisting points from different land types in the same sample [21]. For the creation of these samples, the point cloud has been divided by a grid where each square has the same fixed size of side *N* on the XY axes.

An image (sample) is generated from each square of the grid. The image contains the number of features (pixels) existing in that section of the cloud. The feature extraction is done by rasterization. Rasterization is the process by which it is reduced to the dimensionality of a data set and the points are projected onto a plane (XY in this case). The result of the rasterization of the point cloud $\boldsymbol{P} = (\boldsymbol{P_x}, \boldsymbol{P_y}, \boldsymbol{P_z}, \boldsymbol{In}, \boldsymbol{Nr})$ is an image $\boldsymbol{I} = (\boldsymbol{I_i}, \boldsymbol{I_j})$. This loss of dimension must be matched with a correct choice of features. As in the previous process, a pixel size MxM must be established to arrive at a compromise solution: a small size allows higher resolution of the sample images but must ensure that there are enough points in each pixel to be able to extract features correctly. Fig.1 shows the equivalence between the point cloud in a grid and the image-samples for the train the classifier.

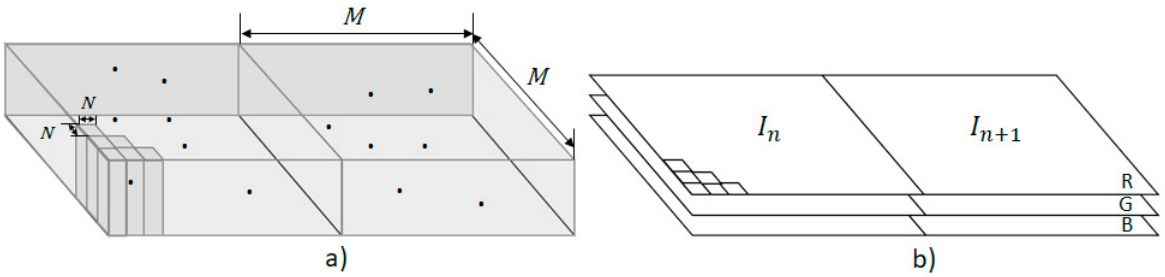

Fig. 1: Equivalence between points cloud ordered by a grid (a) and images-samples for training and classification (b).

The images for training and classification have three channels, RGB images, which allows the extraction of three characteristics, one associated with each channel. The features obtained from the LIDAR data are: height difference of points on each cell in R (Eq.1), mean intensity of points on each cell in G (Eq.2), and mean of the number of average returns of points on each cell in B (Eq. 3). These characteristics, and others similar, have been studied in other works [16] and favor the differentiation between land types. It is important that these features are the most different from each other, not allowing combinations between them, to provide more information to the classifier. The difference in height is a geometric variable and it is greater in urban areas (differences between roofs and ground) and forest areas (treetops and ground). The intensity depends on the reflectivity of the material and it is higher in specific points urban areas and homogeneous according to crops in agricultural areas. The number of returns indicates the ability of the laser to permeate a material, usually associated with vegetation and is high especially in forests. All the features are normalized by a value (N_{Pz}, N_{In}, N_{Nr}) to allow a clearer visualization.

$$R_{ij} = \frac{max(P_z) - min(P_z)}{N_{Pz}} : P \in (I_i, I_j) \quad (1)$$

$$G_{ij} = \frac{\frac{1}{n}\sum_{i=1}^{n} In}{N_{In}} : P \in (I_i, I_j) \quad (2)$$

$$B_{ij} = \frac{\frac{1}{n}\sum_{i=1}^{n} Nr}{N_{Nr}} : P \in (I_i, I_j) \quad (3)$$

3.2 Training and classification

Once the process of generating samples has been carried out, the resulting images can be used to train or be classified. A classifier based on Deep Learning techniques has been chosen to present a great performance in the current state of the art. The use of a classifier based on Deep Learning requires a previous training phase. For the training, representative data labeled from the samples to be classified should be used in a sufficient balanced quantity that allows a good execution of the process. The labeled data is obtained from the current CORINE inventory.

4. Experiments

4.1 Case study

One case study has been selected for the implementation of the methodology. It corresponds to the city of Oviedo (Spain) and its surroundings. The point cloud has 14 million points and covers an area of 17 million square meters. It is available for public download in the website of the "Instituto Geográfico Nacional" [22]. This area has been

chosen because it contains various land types and its acquisition was made in 2012, the same year as the last update of the CORINE inventory. Fig. 2.a shows the point cloud of the study area in real RGB color for easy interpretation (although the color is not used in this work) and Fig. 2.b shows the point cloud colored by CORINE land type.

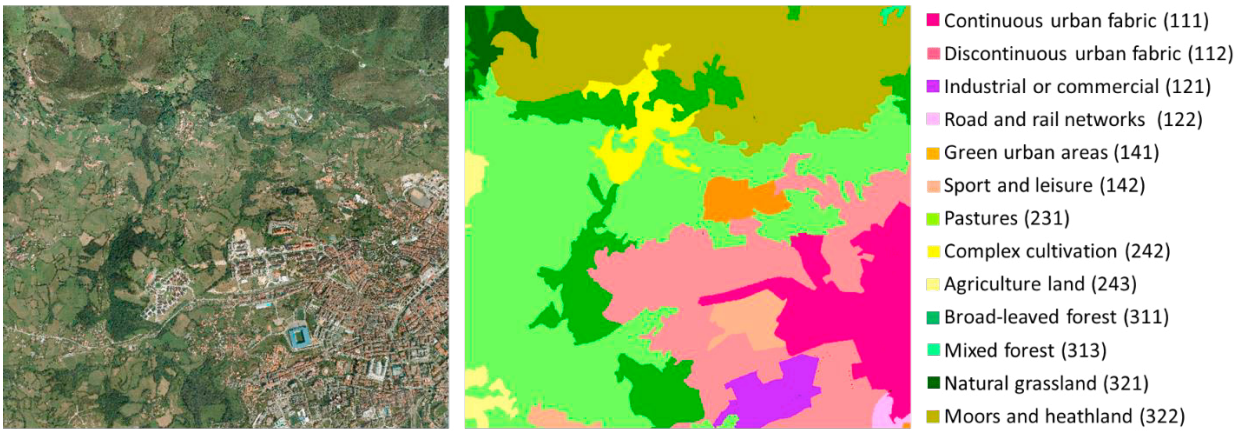

Fig. 2: Point cloud of the Oviedo and surroundings in RGB (a) and colored bay land types (b).

4.2 Sample parameters

The size of the samples for the application of the methodology has been set at M = 50 m, smaller than the minimum replenishment offered by CORINE inventory (500 m). The pixel size is set to N = 2 m, this allows the existence of enough points inside the pixel to extract the features correctly. The point cloud density in this area corresponds to 1,31 points/m^2 (empirically average). The normalization indexes have been set at N_{Pz} = 20 m (height of many trees and buildings) N_{In} = 500 (maximum estimated vegetation reflectivity) and N_{Nr} = 4 (maximum number of returns). Fig. 3 shows separately each of the channels and the complete RGB image.

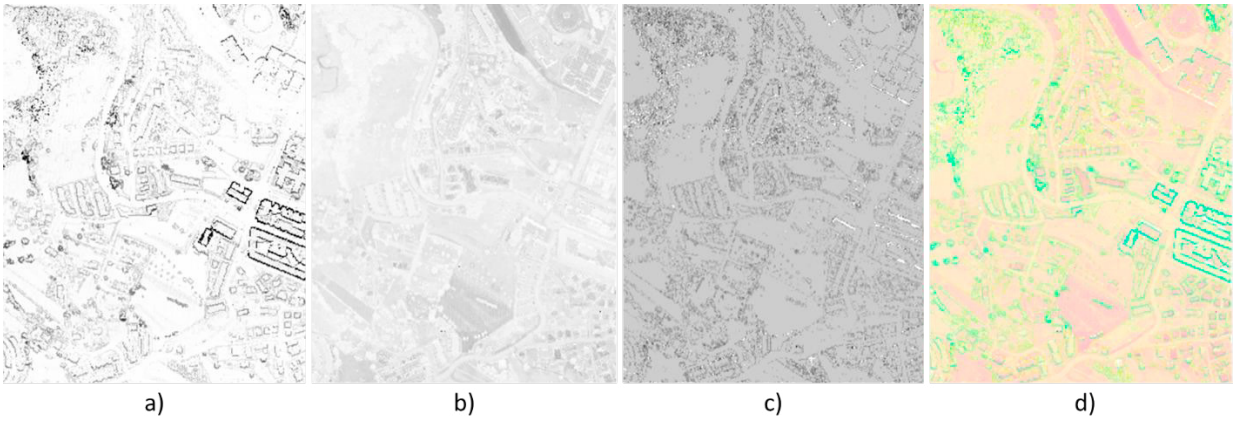

Fig. 3: (a) Image generated based on height (Eq.1), (b) image generated based on intensity (Eq.2), (c) image generated based on number of returns (Eq.3), (d) RGB image generated by joining the previous images and used to train and classify

4.3 Land types

In the study area, there are 13 distinct land types, collected in Table 1 along with their CORINE code, their number of points and their number of equivalent samples. Since the methodology needs to sort the cloud by grouping it into regular square samples, the label of each sample will be the mode of the land types of the existing

points within it. As a result, the number of samples is much smaller than the number of points. The number of samples provided by the study area is clearly unbalanced and many land types do not have enough samples to train a Deep Learning classifier. Due to this, a grouping of typos is established, level 1 classification (first digit of the CORINE code) with three balanced land types: artificial surfaces, agricultural areas, and forest and semi-natural areas. Other options have been discarded, such as grouping around level 2 or the grouping of similar groups, since neither quantities of samples necessary for the training of a neural network are obtained.

Table 1. Land types in the case study.

Land cover	CORINE code	Number of points	Number of samples
Continuous urban fabric	111	1240797	638
Discontinuous urban fabric	112	2329563	1169
Industrial or commercial units	121	344789	168
Road and rail networks and associated land	122	44815	25
Green urban areas	141	229251	113
Sport and leisure facilities	142	235908	139
Pastures	231	4558369	2302
Complex cultivation patterns	242	438890	197
Agriculture land	243	169853	79
Broad-leaved forest	311	1412619	668
Mixed forest	313	21341	9
Natural grassland	321	193601	108
Moors and heathland	322	2886889	1519

4.4 Training

The training has been carried out using the neural network model ResNet-50, that has already proven its good performance in other applications [23]. The sample dataset has been divided interspersed in 50% for training and 25% for validation and 25% for testing (Table 2). The network has been trained in Matlab, with a GPU NVIDIA GTX1050 with 4GB GDDR5, CPU i7-7700HQ 2.8Ghz and 16GB RAM DDR4. The hyperparameters for training are the following: optimization method SGM, learning rate 0.0001, Momentum 0.9, L2 Regularization 0.0001, Max Epochs 20 and Mini Batch Size 8. The time consumed by the training process was 30 minutes. The evolution data of the training are shown in Fig. 4.

Table 2. Balanced land types for classification divided in training, validation and testing.

Land cover	Training	Validation	Testing	Total
Artificial surfaces (1)	1143	554	555	2252
Agricultural areas (2)	1297	640	641	2578
Forest and semi-natural areas (3)	1127	590	587	2304

4.5 Results

From the graph of the training process, it can be seen that there is an increase in accuracy at the beginning but it quickly stagnates at a few iterations. This is a clear indication that the ResNet-50 network is not deep enough to learn the necessary features. The resulting accuracy on the dataset test is 73.5%, while the Cohen Kappa coefficient reaches 59.8% [24], [25]. The results collected in the confusion matrix (Table 3) show a high misclassification rate of land types 1 and 3 towards land type 2 (agricultural areas) and a low index in the opposite direction and between the remaining classes. For a more detailed assessment, a confusion matrix has been made comparing the predicted result in level 1 with the real CORINE land types in level 3 (Table 4). As can be seen, there is no uniform confusion in all land types and certain classes present a greater confusion. Also, those classes with very few samples should be ignored to have representative data. The classes with the most data amount are the ones with the highest relative accuracy (except discontinuous urban fabric). Also, those classes with very few samples that do not become representative should be ignored (road and rail networks and mixed forest).

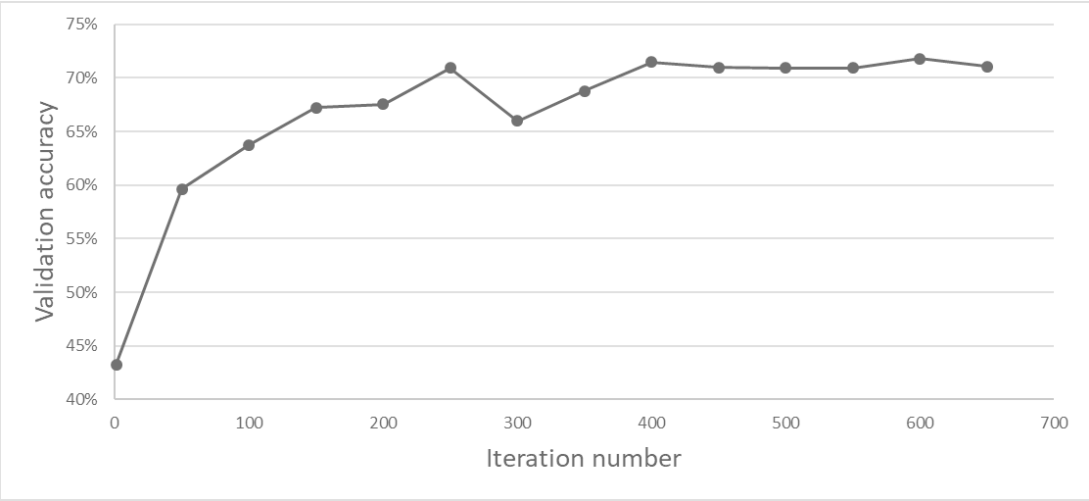

Fig. 4: Evolution of the accuracy during training process.

Table 3. Confusion matrix by land types level 1 for classification with ResNet-50 and images created with point cloud information.

	1	2	3
Artificial surfaces (1)	**330**	196	29
Agricultural areas (2)	14	**554**	73
Forest and semi-natural areas (3)	4	156	**427**

Table 4. Confusion matrix by classified land types level 1 and reference land types level 3 for classification with ResNet-50.

	1	2	3	1 (%)	2 (%)	3 (%)
	Number of samples			Accuracy equivalent		
Continuous urban fabric (111)	**135**	22	2	**84,9%**	13,8%	1,3%
Discontinuous urban fabric (112)	**147**	130	11	**51,0%**	45,1%	3,8%
Industrial or commercial units (121)	**28**	11	1	**70,0%**	27,5%	2,5%
Road and rail networks and associated land (122)	**3**	3	0	**50,0%**	50,0%	0,0%
Green urban areas (141)	**1**	18	11	**3,3%**	60,0%	36,7%
Sport and leisure facilities (142)	**16**	12	4	**50,0%**	37,5%	12,5%
Pastures (231)	14	**505**	54	2,4%	**88,1%**	9,4%
Complex cultivation patterns (242)	0	**33**	14	0,0%	**70,2%**	29,8%
Agriculture land (243)	0	**16**	5	0,0%	**76,2%**	23,8%
Broad-leaved forest (311)	0	28	**140**	0,0%	16,7%	**83,3%**
Mixed forest (313)	0	2	**0**	0,0%	100,0%	**0,0%**
Natural grassland (321)	0	21	**6**	0,0%	77,8%	**22,2%**
Moors and heathland (322)	4	105	**281**	1,0%	26,9%	**72,1%**

The discontinuous urban fabric class is very confused with the agricultural areas (45%). This is due to the fact that these urban areas are open spaces, sometimes groups of villas or land not yet built; in addition, some agricultural areas have numerous single-family homes and low-rise buildings without being considered urban areas. Urban green areas and sports-leisure areas are another sources of confusion with agricultural areas due to the similarity between both classes. The classification of these areas as urban corresponds more with semantic reasons than with data measurable by LIDAR. In the agricultural areas, there is an important confusion between complex cultivation patterns towards forest areas. This is due to the existence of trees among some fields, some crops that can be confused with bushes and abandoned fields. With regard to wooded and natural areas, the greatest confusion is caused by the natural grassland with agricultural areas (22,2% of accuracy and 77,8% of confusion). With regard to wooded and natural areas, the greatest confusion is caused by the natural grassland with agricultural areas. These two areas are extremely difficult to differentiate, even by the human eye. Evaluated all the confusions, it should be

mentioned that there are areas with very low confusion and good relative accuracies, such as the continuous urban fabric (84.9% of accuracy), pastures (88.1%), agriculture lands (76,2%) and broad-leaved forests (83.3%).

4.6 Comparison with deep learning classification using aerial photographs and human classification.

To establish a comparison between the method presented here and classical techniques, the classifier has been trained with orthoimages supplied by the same data source [22] and of the same year in which the inventory was performed for CORINE with a resolution of 0.25 meters per pixel. The study area, size of each sample *M*, distribution among samples for train/dev/test, the network model and training hyperparameters are the same as those used in the previous development. As a result, an accuracy in the test set of 68.6% has been obtained, this is 4.9% worse than the proposed method with point cloud information. The confusion matrix based on the number of samples is shown in Table 5. Although the accuracy of the artificial surfaces suffers a remarkable ascent, one of the agricultural areas suffers a strong descent due to a great confusion with the wooded and natural zones. In contrast, the accuracy of forest and natural areas remains stable.

Table 5. Confusion matrix by land types level 1 for classification with ResNet-50 and orthoimages.

	1	2	3
Artificial surfaces (1)	**426**	59	69
Agricultural areas (2)	59	**348**	234
Forest and semi-natural areas (3)	42	95	**450**

The difficulty of classification between all level 1 land types can be clearly seen when performed by a human observer. The human classification has been carried out by an expert in the field, familiar with the problem of land classification in aerial view. An accuracy of 84.1% has been obtained, distributed in 85.3% for land type 1, 77.1% for land type 2 and 91.0% for land type 3. Given these indices, it can be determined that this is a complex problem even for the human eye due to the high confusion among the different land types that have been described more in detail in section 4.5.

5. Conclusion

A methodology for an automatic land cover classification through the neural network ResNet-50 has been designed. It is based on LIDAR data information labeled with CORINE inventory for classification. The methodology begins with an ordering of the point cloud in regular squares, which allow a subsequent rasterization and feature extraction. Three features are extracted from the point cloud to create the images used by the classifier, one for each RGB channel: maximum height difference between the points that fall in each pixel, average intensity and average return number. The methodology has been tested in one case study when 50% of the data to train the network, 25% to validate and 25% to test. The results of the application obtain a 73.5% accuracy and a Cohen Kappa coefficient of 59.8%, indices very far from of the human classification (accuracy of 84.1%). Although the features extracted from point clouds improve the results obtained with orthoimages (68.6%), the results continue to be insufficient for an application of the current method. There is an important confusion between strongly similar classes, especially the discontinuous urban fabric and natural grassland with agricultural areas.

However, the analysis of the results has shown great potential for the method. There are also land types with high accuracies, such as the continuous urban fabric, pastures and broad broad-leaved forest. Current results are capable of improvement using a deeper neural network, a field of study in constant evolution today, and increasing the number of samples according to the size of the network. Another future action is to obtain images-samples for training and classification with higher resolution increasing its surface area. On the other hand, the use of point clouds, although it requires a longer time and computational cost, is a viable alternative to the use of satellite and aerial images as the three features have shown, providing information not available through other measurement techniques.

Acknowledgements

Authors would like to thank to the *Universidade de Vigo* for the financial support (00VI 131H 641.02), the *Xunta de Galicia* given through human resources grant (ED481B 2016/079-0) and competitive reference groups (ED431C 2016-038), and the *Ministerio de Economia, Industria y Competitividad -Gobierno de España-* (TIN2016-77158-C4-2-R, RTC-2016-5257-7). The statements made herein are solely the responsibility of the authors.

References

[1] E. Kalnay and M. Cai, "Impact of urbanization and land-use change on climate," *Nature*, vol. 423, p. 528, May 2003.
[2] A. Veldkamp and E. F. Lambin, "Predicting land-use change," *Agric. Ecosyst. Environ.*, vol. 85, no. 1, pp. 1–6, 2001.
[3] G. Büttner, J. Feranec, G. Jaffrain, L. Mari, G. Maucha, and T. Soukup, "The CORINE land cover 2000 project," *EARSeL eProceedings*, vol. 3, no. 3, pp. 331–346, 2004.
[4] J. Feranec, G. Hazeu, S. Christensen, and G. Jaffrain, "Corine land cover change detection in Europe (case studies of the Netherlands and Slovakia)," *Land use policy*, vol. 24, no. 1, pp. 234–247, 2007.
[5] J. Feranec, G. Jaffrain, T. Soukup, and G. Hazeu, "Determining changes and flows in European landscapes 1990–2000 using CORINE land cover data," *Appl. Geogr.*, vol. 30, no. 1, pp. 19–35, 2010.
[6] R. M. Haralick, K. Shanmugam, and I. Dinstein, "Textural Features for Image Classification," *IEEE Trans. Syst. Man. Cybern.*, vol. SMC-3, no. 6, pp. 610–621, 1973.
[7] S. Dodge and L. Karam, "A study and comparison of human and deep learning recognition performance under visual distortions," in *Computer Communication and Networks (ICCCN), 2017 26th International Conference on*, 2017, pp. 1–7.
[8] D. Marmanis, M. Datcu, T. Esch, and U. Stilla, "Deep Learning Earth Observation Classification Using ImageNet Pretrained Networks," *IEEE Geosci. Remote Sens. Lett.*, vol. 13, no. 1, pp. 105–109, 2016.
[9] F. P. S. Luus, B. P. Salmon, F. van den Bergh, and B. T. J. Maharaj, "Multiview Deep Learning for Land-Use Classification," *IEEE Geosci. Remote Sens. Lett.*, vol. 12, no. 12, pp. 2448–2452, 2015.
[10] W. Y. Yan, A. Shaker, and N. El-Ashmawy, "Urban land cover classification using airborne LiDAR data: A review," *Remote Sens. Environ.*, vol. 158, pp. 295–310, 2015.
[11] K. K. Singh, J. B. Vogler, D. A. Shoemaker, and R. K. Meentemeyer, "LiDAR-Landsat data fusion for large-area assessment of urban land cover: Balancing spatial resolution, data volume and mapping accuracy," *ISPRS J. Photogramm. Remote Sens.*, vol. 74, pp. 110–121, 2012.
[12] S. Syed, P. H. Dare, and S. Jones, "Automatic Classification of Land Cover Features with High Resolution Imagery and Lidar Data: an Object-oriented Approach," 2005.
[13] B. Koetz, F. Morsdorf, S. van der Linden, T. Curt, and B. Allgöwer, "Multi-source land cover classification for forest fire management based on imaging spectrometry and LiDAR data," *For. Ecol. Manage.*, vol. 256, no. 3, pp. 263–271, 2008.
[14] L. A. Arroyo, K. Johansen, J. Armston, and S. Phinn, "Integration of LiDAR and QuickBird imagery for mapping riparian biophysical parameters and land cover types in Australian tropical savannas," *For. Ecol. Manage.*, vol. 259, no. 3, pp. 598–606, 2010.
[15] M. E. Hodgson, J. R. Jensen, J. A. Tullis, K. D. Riordan, and C. M. Archer, "Synergistic Use of Lidar and Color Aerial Photography for Mapping Urban Parcel Imperviousness." .
[16] N. Chehata, L. Guo, and C. Mallet, "Airborne lidar feature selection for urban classification using random forests," *Int. Arch. Photogramm. Remote Sens. Spat. Inf. Sci.*, vol. 38, no. Part 3, p. W8, 2009.
[17] Z. Chen and B. Gao, "An Object-Based Method for Urban Land Cover Classification Using Airborne Lidar Data," *IEEE J. Sel. Top. Appl. Earth Obs. Remote Sens.*, vol. 7, no. 10, pp. 4243–4254, 2014.
[18] J. S. Yoon, J. I. Shin, and K. S. Lee, "Land Cover Characteristics of Airborne LiDAR Intensity Data: A Case Study," *IEEE Geosci. Remote Sens. Lett.*, vol. 5, no. 4, pp. 801–805, 2008.
[19] A. S. Antonarakis, K. S. Richards, and J. Brasington, "Object-based land cover classification using airborne LiDAR," *Remote Sens. Environ.*, vol. 112, no. 6, pp. 2988–2998, 2008.
[20] W. Zhou, "An Object-Based Approach for Urban Land Cover Classification: Integrating LiDAR Height and Intensity Data," *IEEE Geosci. Remote Sens. Lett.*, vol. 10, no. 4, pp. 928–931, 2013.
[21] S. W. Myint, P. Gober, A. Brazel, S. Grossman-Clarke, and Q. Weng, "Per-pixel vs. object-based classification of urban land cover extraction using high spatial resolution imagery," *Remote Sens. Environ.*, vol. 115, no. 5, pp. 1145–1161, 2011.
[22] Centro Nacional de Información Geográfica, "Centro de descargas." [Online]. Available: www.centrodedescargas.cnig.es. [Accessed: 19-Jan-2018].
[23] K. He, X. Zhang, S. Ren, and J. Sun, "Deep residual learning for image recognition," in *Proceedings of the IEEE conference on computer vision and pattern recognition*, 2016, pp. 770–778.
[24] K. J. Berry and J. Paul W. Mielke, "A Generalization of Cohen's Kappa Agreement Measure to Interval Measurement and Multiple Raters," *Educ. Psychol. Meas.*, vol. 48, no. 4, pp. 921–933, Dec. 1988.
[25] A. J. Tallón-Ballesteros and J. C. Riquelme, "Data Mining Methods Applied to a Digital Forensics Task for Supervised Machine Learning BT - Computational Intelligence in Digital Forensics: Forensic Investigation and Applications," A. K. Muda, Y.-H. Choo, A. Abraham, and S. N. Srihari, Eds. Cham: Springer International Publishing, 2014, pp. 413–428.